

Composite dynamics in $\text{Sp}(2N)$ gauge theories

Jong-Wan Lee^{1,2,*}, Ed Bennett³, Deog Ki Hong¹, Ho Hsiao⁴, C.-J. David Lin^{4,5}, Biagio Lucini^{3,6}, Maurizio Piai⁷, and Davide Vadacchino⁸

¹Department of Physics, Pusan National University, Busan 46241, Korea

²Institute for Extreme Physics, Pusan National University, Busan 46241, Korea

³Swansea Academy of Advanced Computing, Swansea University (Bay Campus), Fabian Way, SA1 8EN Swansea, Wales, United Kingdom

⁴Institute of Physics, National Yang Ming Chiao Tung University, 1001 Ta-Hsueh Road, Hsinchu 30010, Taiwan

⁵Center for High Energy Physics, Chung-Yuan Christian University, Chung-Li 32023, Taiwan

⁶Department of Mathematics, Faculty of Science and Engineering, Swansea University (Bay Campus), Fabian Way, SA1 8EN Swansea, Wales, United Kingdom

⁷Department of Physics, Faculty of Science and Engineering, Swansea University (Park Campus), Singleton Park, SA2 8PP Swansea, Wales, United Kingdom

⁸Centre for Mathematical Science, University of Plymouth, Plymouth, PL4 8AA, United Kingdom

Abstract. $\text{Sp}(2N)$ gauge theories with fermionic matter provide an ideal laboratory to build extensions of the standard model based on novel composite dynamics. Examples include composite Higgs along with top partial compositeness and composite dark matter. Without fermions, their study also complements those based on $\text{SU}(N_c)$ gauge theories with which they share a common sector in the large $N_c = 2N$ limit. We report on our recent progress in the numerical studies of $\text{Sp}(2N)$ gauge theories discretised on a four-dimensional Euclidean lattice. In particular, we present preliminary results for the low-lying mass spectra of mesons and chimera baryons in the theories with $N = 2$. We also compute the topological susceptibility for various values of N , extrapolate the results to the large N limit, and discuss certain universal properties in Yang-Mills theories.

1 Introduction

Non-abelian gauge theories based on $\text{Sp}(N_c = 2N)$ groups coupled to fermions exhibit interesting nonperturbative phenomena, such as confinement and global symmetry breaking, analogous to the $\text{SU}(N_c)$ gauge theories. In Yang-Mills theories, they provide another family of groups in which certain universal features are expected to emerge in the large N_c limit. In the opposite extreme limit we have $\text{SU}(2) = \text{Sp}(2)$. A distinctive feature is that the fundamental representation of $\text{Sp}(2N)$ is pseudoreal. When the gauge dynamics is coupled to N_f fundamental Dirac flavours, the main consequences are two-fold. On the one hand, finite density calculations are free from the *sign problem*, a notorious hindrance in the numerical studies of QCD, and thus may provide new physical insights on the phase diagram. On the other hand, the global symmetry associated with the flavour is enhanced to $\text{SU}(2N_f)$, which

*e-mail: jwlee823@pusan.ac.kr

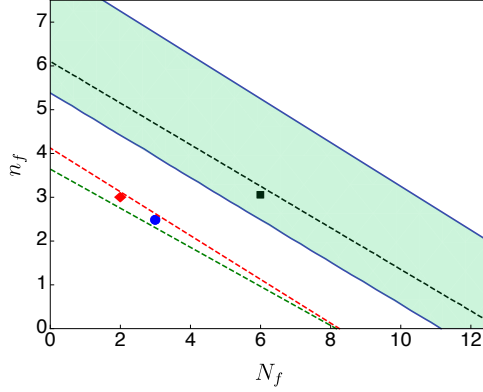


Figure 1. Phase diagram of $\text{Sp}(4)$ gauge theory with N_f fundamental and n_f antisymmetric Dirac fermions. The shaded region denotes the conformal window recently estimated in Ref. [2], while dashed lines denote other analytical estimations in the literature, which are discussed in the same reference. The coloured dots represent the theories realising the phenomenological models discussed in the main text.

is spontaneously and explicitly broken into $\text{Sp}(2N_f)$ in the presence of fermion condensation and non-zero (degenerate) mass. Because such a symmetry breaking pattern yields a comparatively large coset space, one can take advantage of it when constructing certain classes of phenomenological extensions of the standard model (SM), such as composite Higgs, top partial compositeness, and a strongly interacting massive particle (SIMP) as dark matter candidate. Furthermore, it is known that the finite-temperature transition of pure $\text{Sp}(2N)$ gauge theories is first order for $N \geq 2$ [1], which has a potential impact on studies of the cosmological evolution of the early universe and on gravitational wave experiments. It should be emphasized that, in principle, $\text{Sp}(2N)$ gauge theories are equally important as $\text{SU}(N_c)$ in the searches for new physics based on novel strongly coupled gauge theories.

To perform lattice simulation, we need to choose a concrete model, well motivated by both theoretical and phenomenological arguments. We concentrate on the minimal $\text{Sp}(4)$ theory with which one can build both composite Higgs and top partial compositeness. In Fig. 1, we show the theory space of $\text{Sp}(4)$ with N_f fundamental and n_f 2-index antisymmetric Dirac fermions. Representative models taken from the literature are denoted by red [3, 4], blue [4] and black [5] colours. As the infrared (IR) behaviour of strongly coupled gauge theories determines what type of applications they suit, in the figure we also present the results of a recent analytical study of the edge of the conformal window (CW), compared with other analytical estimations (see Ref. [2] and references therein for the details).

The theory with $N_f = 2$ fundamental and $n_f = 3$ antisymmetric Dirac fermions is expected to be in the chirally broken phase. The resulting 5 pseudo Nambu-Goldstone bosons (pNGBs) in the fundamental sector include the SM Higgs doublets. This theory can be studied by employing currently available numerical lattice techniques without altering the flavour structure of the original, phenomenologically motivated model. Since numerical studies of gauge theories with mixed representations are relatively new to the lattice community, and computationally demanding in the presence of dynamical fermions, we have first considered the quenched approximation [6, 7] and in stages introduced dynamical Dirac flavours in the form of two fundamental [8], three antisymmetric [9] and both combined [10].

In parallel, we have been studying pure $\text{Sp}(2N)$ gauge theories on the lattice with various values of N , $N = 1, 2, 3, 4$, and furthermore considered the extrapolation towards the large

N limit. We have studied the string tension, the mass spectra of glueballs with many different quantum numbers (including some excited states) [11], the Wilson flow and the topological susceptibility [12], and found empirical evidence of the emergence of universal patterns in Yang-Mills theories [13–15].

2 Lattice setup

The lattice action of $\text{Sp}(2N)$ gauge theories is discretised in a four-dimensional Euclidean space with temporal and spatial extents T and L , respectively. We adopt the standard plaquette action for pure gauge interactions and the Wilson-Dirac action for gauge-fermion interactions. Details can be found in Refs. [10, 12] and references therein. Numerical calculations have been carried out by employing the Heat Bath algorithms for the pure $\text{Sp}(2N)$ theories and the (rational) hybrid Monte Carlo algorithms for the $\text{Sp}(4)$ theories with dynamical fermions. The lattice action contains a lattice coupling $\beta \equiv 4N/g^2$ and fermion masses am_0^f and am_0^{as} for the fundamental and antisymmetric representations, respectively. Here, g is the bare gauge coupling and a is the lattice spacing.

The lattice parameters need to be chosen carefully so that the lattice measurements can be extrapolated to the corresponding continuum ones by taking $\beta \rightarrow \infty$ in a controlled way. In particular, we investigated the presence of a first-order bulk phase transition and, if it exists, determined the critical coupling β^c associated with the boundary between strong and weak coupling regimes. We have shown that $\text{Sp}(2N)$ Yang-Mills for $N = 1, 2, 3, 4$ exhibits a smooth crossover [11], while dynamical $\text{Sp}(4)$ theories undergo a first-order transition in the strong coupling regime [6, 10, 16]. Having the values of β^c in hand, we have performed all the numerical simulations in the weak coupling regime, $\beta > \beta^c$, and extrapolated to the continuum, if possible. Furthermore, we have used choices of the lattice volume for which finite size corrections to the observables are statistically negligible. We elected to set a scale for dimensionful quantities by using the gradient flow method [17]. Two different definitions of the flow scale, t_0 [17] and w_0 [18], are available. Furthermore, the string tension σ can be used in the case of pure $\text{Sp}(2N)$ Yang-Mills.

3 Results: $\text{Sp}(2N)$ Yang-Mills

In this section, we briefly summarise our main findings on $\text{Sp}(N_c = 2N)$ pure gauge theories with $N = 1, 2, 3, 4$ and discuss certain universal features in Yang-Mills theories by comparing to $\text{SU}(N_c)$ and $\text{SO}(N_c)$ gauge theories. We refer the reader to Refs. [11, 12, 14, 15] for the full details of lattice technicalities and numerical results.

Two main observables are the mass of glueballs and the string tension, which are extracted from the large-time behaviour of the 2-point correlation functions built out of Wilson and Polyakov loops, respectively. Two-point functions involving Polyakov loops have been measured to extract the string tension. The masses of glueballs are obtained by studying a variational problem involving correlators between two Wilson loops of various shapes and sizes. The spin quantum numbers J of the glueball states in the continuum theory are determined through the decomposition of the irreducible representations of the octahedral group—the symmetry group of a cubic lattice—in the lattice theory. Using variational techniques, we were able to extract the masses for the ground states with $J^P = 0^\pm, 1^\pm, 2^\pm, 3^\pm$ as well as for the first excited states with 0^\pm [11]. After performing the continuum extrapolations of the glueball masses in units of $\sqrt{\sigma}$ at each N_c , we took the large N_c limit by including a $\mathcal{O}(1/N_c)$ correction term. We found that the resulting values at $N_c = \infty$ are in good agreement with those for $\text{SU}(N_c)$ [11, 19]. We also note that the lightest and the second lightest states are the positive-parity scalar and tensor glueballs.

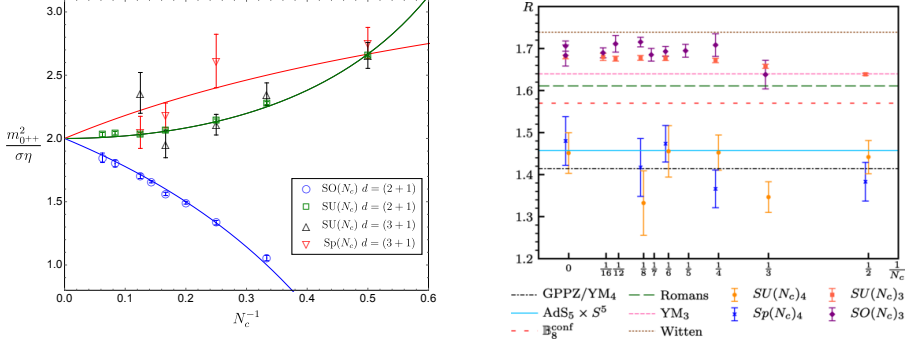


Figure 2. Numerical results and extrapolations towards the large N_c limit, showing the convergence of the $SU(N_c)$, $Sp(N_c)$ and $SO(N_c)$ Yang-Mills theories: (left) Casimir scaling in the lightest scalar glueballs, and (right) mass ratio between the lightest scalar and tensor glueballs, $R \equiv m_{2^{++}}/m_{0^{++}}$. The constant η is defined in Eq. (1). Figures from Refs. [11, 13, 14].

Recently, it has been argued that certain ratios between physical observables, up to appropriate gauge-group factors, might exhibit universal behaviours even at finite N_c in $SU(N_c)$, $Sp(N_c)$ and $SO(N_c)$ Yang-Mills [13, 20]. Here, *universal* means that the ratio only depends on the space-time dimension of the theory, d , regardless of the number of colours N_c and the gauge groups. First of all, in Ref. [13] the authors conjectured that the ratio $m_{0^{++}}^2/\sigma$ is proportional to the ratio of eigenvalues of quadratic Casimir operators in the adjoint (Adj) and the fundamental (F) representations, which is supported by existing lattice results for $SO(N_c)$ in $d = (2+1)$ and $SU(N_c)$ in both $d = (2+1)$ and $(3+1)$ theories. Combining our results for $Sp(N_c)$, as shown in Fig. 2, we obtained the following results for the universal constant η [11, 13]

$$\eta \equiv \frac{m_{0^{++}}^2}{\sigma} \cdot \frac{C_2(F)}{C_2(Adj)} = \begin{cases} 5.388(81)(60), & d = (3+1), \\ 8.440(14)(76), & d = (2+1), \end{cases} \quad (1)$$

where the first and second parentheses denote the statistical and systematic errors, respectively.

A second interesting quantity is the mass ratio between the lightest parity-even scalar and tensor glueballs, $R \equiv m_{2^{++}}/m_{0^{++}}$, first proposed in Ref. [20]. In Fig. 2, we present the lattice results available in the literature as well as analytical results obtained by gauge-gravity dualities and field-theoretical calculations. Details are found in Ref. [14]. As seen in the figure, it is evident that the ratio R is independent of N_c and the gauge group, but gives rise to different values for $d = (2+1)$ and $(3+1)$ dimensions.

An interesting non-perturbative quantity, which is closely related with the $U(1)_A$ problem and the θ -term, is the topological susceptibility χ . Since χ is defined as a second derivative of the vacuum density $F(\theta)$ with respect to θ , and each gauge field contributes equally, it has been conjectured to be proportional to the dimension of group d_G . We hence investigate the behaviour of the ratio $\eta_\chi \equiv \chi C_2(F)^2/\sigma^2 d_G$ [15]. A survey of lattice results for $d = (3+1)$ $SU(N_c)$ and $Sp(N_c)$ Yang-Mills can be found in Fig. 3. While the two sequences of gauge groups agree with each other, we observe a visible dependence on d_G . After accounting for the N_c dependence, we took the large- N_c extrapolation and obtained [15]:

$$\eta_\chi(N_c = \infty) = 48.4(8)(33) \times 10^{-4}, \quad (2)$$

where the first and second parentheses again denote the statistical and the systematic errors.

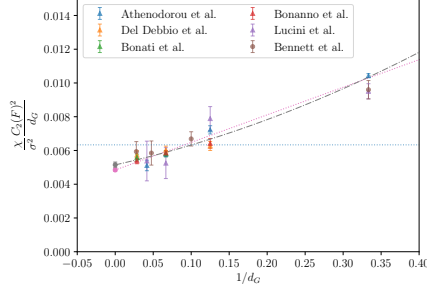


Figure 3. Topological susceptibilities χ in units of the string tension σ , rescaled by group factors $C_2(F)^2/d_G$, for $SU(N_c)$ and $Sp(N_c)$ Yang-Mills as a function of the dimension of the group d_G . The figure is taken from Ref. [15].

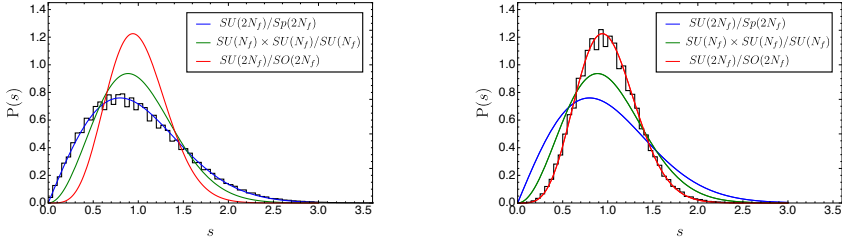


Figure 4. The unfolded density of the spacings between subsequent Dirac eigenvalues for the fundamental (left) and antisymmetric (right) representations. The black histogram denotes the numerical data, while the coloured solid lines are the χ RMT predictions. Figures from Ref. [10].

4 Results: $Sp(4)$ with fermions

We restrict ourselves to the $Sp(4)$ gauge group for the cases involving fermionic matter fields. Because these are the first numerical studies of fermions in the fundamental and antisymmetric representations transforming under $Sp(2N)$ with $N \geq 2$, we have performed nontrivial tests of the algorithms. A particularly important cross-check pertains the breaking pattern of the flavour symmetry. Following the work in Ref. [21], we calculated the eigenvalues of the Dirac operators in the quenched ensemble on a small lattice of size 4^4 , and compared the unfolded density of spacings, $P(s)$, with the predictions of chiral random matrix theory (χ RMT) [10]. As seen in Fig. 4, the histograms of our numerical data are well described by the χ RMT predictions, denoted as solid lines, with the expected breaking patterns of $SU(2N_f)/Sp(2N_f)$ and $SU(2N_f)/SO(2N_f)$ for the fundamental and antisymmetric fermions, respectively.

We now turn our attention to the results for dynamical fermions. In Ref. [8], we reported the spectral results for flavoured mesons in the lightest spin-0 and -1 channels, measured on dynamical ensembles with $N_f = 2$ fundamental Dirac fermions. We examined the fermion mass dependence of the mass and decay constant of pseudoscalar meson, the lightest state in the spectrum, and found clear evidence of the spontaneous breaking of the global symmetry: the mass squared is proportional to the fermion mass and the decay constant extrapolates to a non-zero value in the massless limit. This is expected by the fact that the pNGBs span the $SU(4)/Sp(4)$ coset relevant for models of composite Higgs and SIMP dark matter. Concerning the theory with $n_f = 3$ antisymmetric Dirac fermions, we also found some evidence of the

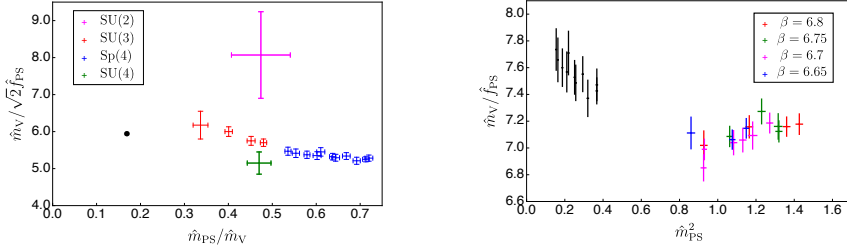


Figure 5. (left) Vector meson masses in various gauge theories with $N_f = 2$ fundamental Dirac flavours: different colours are for various gauge groups, while the black dot denotes the QCD value. (right) Vector meson masses in Sp(4) theory with $N_f = 2$ fundamental (in the continuum, black) and $n_f = 3$ antisymmetric (colours for different β values) Dirac flavours. The hatted notation denotes the mass in units of the gradient flow scale, w_0 , e.g. $\hat{m}_{PS} = m_{PS} w_0$. Figures are taken from Refs. [8, 9].

spontaneous beaking of the global symmetry in our preliminary results [9], which need to be further confirmed by extending the calculations to smaller fermion mass. In the case of a fully dynamical Sp(4) theory with both two fundamental and three antisymmetric fermions, we have carried out lattice studies on a single ensemble so far [10], and thus cannot yet make any statement on its IR nature.

The lightest state in the spin-1 channel is the vector meson. Its mass is expected to be non-zero in the massless limit. A particularly interesting quantity is its mass in units of the pseudoscalar decay constant, $m_V / \sqrt{2} f_{PS}$, which is closely related with the low-energy constant associated with its decay to two pseudoscalar mesons via the phenomenological KSFR relation [22, 23]. In Fig. 5, we show our results for the $N_f = 2$ fundamental Sp(4) theory in the continuum limit, compared to other gauge theories [8]. The resulting masses are below the threshold of the two-pseudoscalar decay, yet our results indicate a value for the ratio in Sp(4) that is somewhere between SU(3) and SU(4) theories near the threshold.

The right panel of Fig. 5 shows our preliminary results for the same ratio for the $n_f = 3$ antisymmetric Sp(4) theory measured at different β values. For comparison, we also present the continuum results of the $N_f = 2$ fundamental Sp(4) theory. Although a direct comparison may not be possible due to the different mass range (and the absence so far of a continuum extrapolation in the former case), we can see that the former is slightly smaller than the latter. This result is consistent with large- N_c argument: m_V is independent on the representation while f_{PS}^2 is proportional to the dimension of the representation. A survey of the lattice results of m_V / f_{PS} for various gauge theories, e.g. different numbers of colours and flavours, and different gauge groups and fermion representations, can be found in Ref. [24].

The most interesting and distinct feature of gauge theories with mixed representations is the existence of colour-singlet baryonic objects, dubbed *chimera* baryons, some of which have the same SM quantum numbers of the top quark. In modern scenarios of composite Higgs, in particular, this feature is exploited to explain the large mass of the top quark, through partial compositeness. In the Sp(4) theory considered in this work, the interpolating operators for the chimera baryons can be constructed from two fundamental and one antisymmetric fermion constituents. Even though the colour contraction and the flavour symmetry are completely different from QCD, the structure of these operators is similar to that for the QCD baryons involving one heavy quark. More explicitly, we label the lightest spin-1/2 and 3/2 chimera states, $(J, R) = (1/2, 5)$, $(1/2, 10)$ and $(3/2, 10)$ by Λ , Σ and Σ^* , respectively, where, J and R denote the spin and the irreducible representation of the flavour group acting on the fundamental fermions.

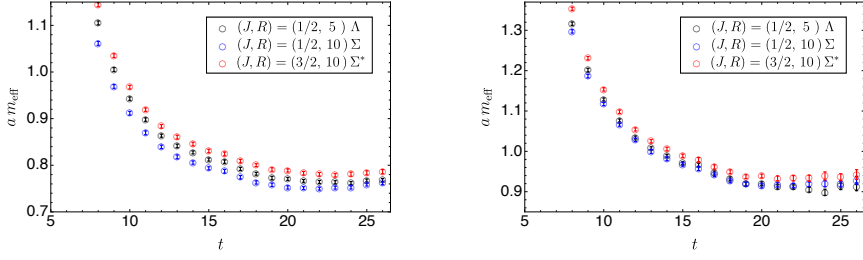


Figure 6. Effective mass plots for the lightest spin-1/2 and 3/2 chimera baryons in partially quenched approximation. The details of the ensemble can be found in Ref. [10]. The valence fermions masses are $(am_v^f, am_v^{as}) = (-0.71, -1.01)$ and $(-0.75, -0.8)$ for the left and right panels, respectively.

We refer the reader to Refs. [10, 25] for details on the interpolating operators, the parity and spin projections, the measurements, and exploratory studies of the spectrum. One observation we immediately made from our preliminary studies, using the dynamical ensemble with $(\beta, am_0^f, am_0^{as}) = (6.5, -0.71, -1.01)$, was that Λ , being a natural choice of top partner, e.g. Ref. [26] (but, see also Ref. [27] for the other possibilities), is not the lightest state, as shown in the left panel of Fig. 6. To further investigate the mass hierarchy of chimera baryons, we performed additional measurements in a partially quenched setup using the same ensemble—the valence fermion mass is different to the sea fermion, $m_v^{f,as} \neq m_0^{f,as}$. With the choices of $(am_v^f, am_v^{as}) = (-0.75, -0.8)$, we find that the mass ratio between pseudoscalar mesons composed of antisymmetric and fundamental constituents $m_{\text{ps}}^{as}/m_{\text{ps}}^f$ is about 4.3, and Λ is almost degenerate with Σ and thus the lightest state in the baryon spectrum. A similar behaviour has been observed in the quenched approximation [25].

Acknowledgements - We thank Gabriele Ferretti for useful communications. The work of J. W. L is supported by the National Research Foundation of Korea (NRF) grant funded by the Korea government (MSIT) (NRF-2018R1C1B3001379). The work of E. B. has been funded in part by the UKRI Science and Technology Facilities Council (STFC) Research Software Engineering Fellowship EP/V052489/1. The work of D. K. H. was supported by Basic Science Research Program through the National Research Foundation of Korea (NRF) funded by the Ministry of Education (NRF-2017R1D1A1B06033701). The work of H. H. and C. J. D. L. is supported by the Taiwanese MoST Grant No. 109-2112-M-009 -006 -MY3. The work of B. L. and M. P. has been supported in part by the STFC Consolidated Grants No. ST/P00055X/1 and No. ST/T000813/1. B. L. and M. P. received funding from the European Research Council (ERC) under the European Union’s Horizon 2020 research and innovation program under Grant Agreement No. 813942. The work of B. L. is further supported in part by the Royal Society Wolfson Research Merit Award No. WM170010 and by the Leverhulme Trust Research Fellowship No. RF-2020-4619. The work of D. V. is supported in part the Simons Foundation under the program “Targeted Grants to Institutes” awarded to the Hamilton Mathematics Institute. Numerical simulations have been performed on the Swansea SUNBIRD cluster (part of the Supercomputing Wales project) and AccelerateAI A100 GPU system, on the local HPC clusters in Pusan National University (PNU) and in National Yang Ming Chiao Tung University (NYCU), and on the DiRAC Data Intensive service at Leicester. The Swansea SUNBIRD system and AccelerateAI are part funded by the European Regional Development Fund (ERDF) via Welsh Government. The DiRAC Data Intensive service at Leicester is operated by the University of Leicester IT Services, which forms part of the STFC DiRAC HPC Facility (www.dirac.ac.uk). The DiRAC Data Intensive service equipment at Leicester was funded by BEIS capital funding via STFC capital grants ST/K000373/1 and ST/R002363/1 and STFC DiRAC Operations grant ST/R001014/1. DiRAC is part of the National e-Infrastructure.

References

- [1] K. Holland, M. Pepe, U.J. Wiese, Nucl. Phys. B **694**, 35 (2004), hep-lat/0312022
- [2] B.S. Kim, D.K. Hong, J.W. Lee, Phys. Rev. D **101**, 056008 (2020), 2001.02690
- [3] J. Barnard, T. Gherghetta, T.S. Ray, JHEP **02**, 002 (2014), 1311.6562
- [4] G. Ferretti, JHEP **06**, 107 (2016), 1604.06467
- [5] G. Cacciapaglia, S. Vatan, C. Zhang, Phys. Lett. B **815**, 136177 (2021), 1911.05454
- [6] E. Bennett, D.K. Hong, J.W. Lee, C.J.D. Lin, B. Lucini, M. Piai, D. VDACCHINO, JHEP **03**, 185 (2018), 1712.04220
- [7] E. Bennett, D.K. Hong, J.W. Lee, C.J.D. Lin, B. Lucini, M. Mesiti, M. Piai, J. Rantaharju, D. VDACCHINO, Phys. Rev. D **101**, 074516 (2020), 1912.06505
- [8] E. Bennett, D.K. Hong, J.W. Lee, C.J.D. Lin, B. Lucini, M. Piai, D. VDACCHINO, JHEP **12**, 053 (2019), 1909.12662
- [9] J.W. Lee, E. Bennett, D.K. Hong, H. Hsiao, C.J.D. Lin, B. Lucini, M. Piai, D. VDACCHINO, PoS **LATTICE2022**, 214 (2022), 2210.08154
- [10] E. Bennett, D.K. Hong, H. Hsiao, J.W. Lee, C.J.D. Lin, B. Lucini, M. Mesiti, M. Piai, D. VDACCHINO, Phys. Rev. D **106**, 014501 (2022), 2202.05516
- [11] E. Bennett, J. Holligan, D.K. Hong, J.W. Lee, C.J.D. Lin, B. Lucini, M. Piai, D. VDACCHINO, Phys. Rev. D **103**, 054509 (2021), 2010.15781
- [12] E. Bennett, D.K. Hong, J.W. Lee, C.J.D. Lin, B. Lucini, M. Piai, D. VDACCHINO, Phys. Rev. D **106**, 094503 (2022), 2205.09364
- [13] D.K. Hong, J.W. Lee, B. Lucini, M. Piai, D. VDACCHINO, Phys. Lett. B **775**, 89 (2017), 1705.00286
- [14] E. Bennett, J. Holligan, D.K. Hong, J.W. Lee, C.J.D. Lin, B. Lucini, M. Piai, D. VDACCHINO, Phys. Rev. D **102**, 011501 (2020), 2004.11063
- [15] E. Bennett, D.K. Hong, J.W. Lee, C.J.D. Lin, B. Lucini, M. Piai, D. VDACCHINO, Phys. Lett. B **835**, 137504 (2022), 2205.09254
- [16] J.W. Lee, E. Bennett, D.K. Hong, C.J.D. Lin, B. Lucini, M. Piai, D. VDACCHINO, PoS **LATTICE2018**, 192 (2018), 1811.00276
- [17] M. Lüscher, JHEP **08**, 071 (2010), [Erratum: JHEP 03, 092 (2014)], 1006.4518
- [18] S. Borsanyi et al., JHEP **09**, 010 (2012), 1203.4469
- [19] B. Lucini, E. Bennett, J. Holligan, D.K. Hong, H. Hsiao, J.W. Lee, C.J.D. Lin, M. Mesiti, M. Piai, D. VDACCHINO, EPJ Web Conf. **258**, 08003 (2022), 2111.12125
- [20] A. Athenodorou, E. Bennett, G. Bergner, D. Elander, C.J.D. Lin, B. Lucini, M. Piai, JHEP **06**, 114 (2016), 1605.04258
- [21] G. Cossu, L. Del Debbio, M. Panero, D. Preti, Eur. Phys. J. C **79**, 638 (2019), 1904.08885
- [22] K. Kawarabayashi, M. Suzuki, Phys. Rev. Lett. **16**, 255 (1966)
- [23] Riazuddin, Fayyazuddin, Phys. Rev. **147**, 1071 (1966)
- [24] D. Nogradi, L. Szikszai, PoS **LATTICE2019**, 237 (2019), 1912.04114
- [25] H. Hsiao, Bennett, D.K. Hong, J.W. Lee, C.J.D. Lin, B. Lucini, M. Piai, D. VDACCHINO (2022), 2211.03955
- [26] B. Gripaos, A. Pomarol, F. Riva, J. Serra, JHEP **04**, 070 (2009), 0902.1483
- [27] A. Banerjee, D.B. Franzosi, G. Ferretti, JHEP **03**, 200 (2022), 2202.00037